Global NEST Journal, Vol 24, No X, pp 1-8

High selectivity and adsorption capacity for congo red toward anionic dyes by adsorbent: modified LDH with hydrochar made from *Nephelium Lappaceum Peel*

Hasanah M.[1,2], Normah[3], Wijaya A.[4], Arsad F.S.[5], Mohadi R.[2] and Lesbani A.[2,4*]

[1]Department of Pharmacy, School of Pharmacy Bhakti Pertiwi, Palembang 30128, Indonesia
[2]Graduate School of Faculty Mathematics and Natural Sciences, Sriwijaya University, Palembang, 30128, Indonesia
[3]Magister Programme Graduate School of Mathematics and Natural Sciences, Sriwijaya University, Palembang, 30128, Indonesia
[4]Research Center of Inorganic Materials and Coordination Complexes, Faculty of Mathematics and Natural Sciences, Sriwijaya University, Palembang, 30128, Indonesia
[5]Departement of Physical, Faculty of Mathematics and Natural Sciences, Sriwijaya University, Palembang, 30128, Indonesia
Received: 19/03/2022, Accepted: 12/08/2022, Available online: 08/09/2022
*to whom all correspondence should be addressed: e-mail: aldeslesbani@pps.unsri.ac.id
https://doi.org/10.30955/gnj.004306

Graphical abstract

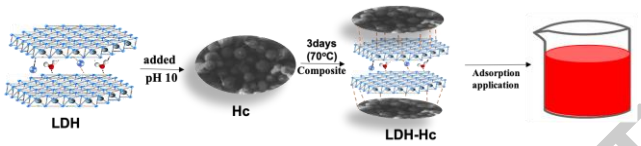

Abstract

Synthesis of Ni/Al-LDH prepared into Ni/Al-Hc composites using hydrochar from rambutan peel (Hc) and applied as a congo red adsorbent and analyzed based on adsorption selectivity, kinetics, isotherms, adsorption thermodynamics and recycling. The success of Ni/Al-Hc composite preparation was proven by XRD, FT-IR, and BET analysis which showed the unique characteristics of Ni/Al and Hc. The results of the analysis of adsorbent characterization using XRD showed that the peaks in the Ni/Al-Hc composite were similar to typical peaks of Ni/Al appearing around 10.9°(003), 45.5°(018) and hydrochar appearing around 22°(002). The results of the analysis were strengthened by characterization using FT-IR which showed that the Ni/Al-Hc composite had similar spectra with the precursor. BET analysis showed that the Ni/Al-Hc composite had an increase in specific surface area to 11.879 m^2/g from 5.845 m^2/g after Ni/Al was composited with Hc. The adsorption study showed that the Ni/Al-Hc composite showed selective ability to congo red, and was in equilibrium at 100 minutes with a tendency for adsorption to follow pseudo first order (R^2 is closer to 1). The adsorption isotherm shows that the adsorption of Congo red tends to follow Freundlich with the maximum adsorption capacity reaching qm (adsorption capacity) of 246.23 mg/g each using Ni/Al-Hc adsorbent and the adsorption process takes place by spontaneous and endothermic. The adsorption regeneration ability is more stable up to the fourth cycle compared to Ni/Al-LDH and Hc with the best desorption reagent using hydrochloric acid.

Keywords: Modified LDH, Hydrochar, Adsorption, Congo Red, Regeneration

1. Introduction

Congo red (CR) dye has been widely used in the , paper, textile, printing, rubber, and dyeing, (Mishra *et al.,* 2020). Congo red found in the environment and hydrosphere is highly carcinogenic to humans and living organisms and will damage environmental ecosystems (Adebayo *et al.,* 2016). Congo red is a representative anionic diazo dye due to its persistence in the environment and its high solubility in aqueous and carcinogenic (Adebayo *et al.,*2016). It is very difficult to remove industrial waste dyes, because dyes are not easily degraded naturally in the environment and Congo Red is a dye that has a stable structure (Figure 1).

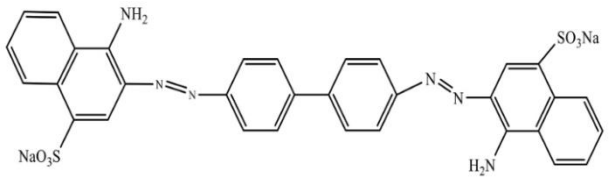

Figure 1. Strucuture Congo Red.

Conventional technology to remove congo red dye from industrial waste such as chemical, biological and physicochemical methods (Chisutia *et al.,* 2014; Devi *et al.,* 2020; S. Li *et al.,* 2020; Litefti *et al.,* 2019; Ma *et al.,* 2021; Olusegun and Mohallem, 2020). Methods that can be used are filtration, photocatalysis, ion exchange, electrochemical oxidation, biological treatment and adsorption (Adeyemo *et al.,* 2017; Li *et al.,* 2020; Satya *et al.,* 2020). Among these methods, adsorption was found

to be the more effective and most promising method so that it is widely used because of its simple setup, low cost, high efficiency and very small by-product formation. One of the adsorbents that can be used is biomass-based activated carbon. This is because activated carbon exhibits competitive adsorption properties and the potential for low cost, high efficiency, simplicity of design, and operation resulting in high adsorption performance, porous structure, easy modification with other materials and large specific surface area. Various literature studies report that carbon-based materials can be made with various agricultural wastes such as durian peel (Ayu *et al.,*2020), orange peel (Xie *et al.,* 2014), banana peel (Viena *et al.,* 2019), rice husk (Palapa *et al.,* 2021) , algae, sludge (Nazal n.d.), and rambutan peel (Normah *et al.,* 2021).

Rambutan (*Nephelium lappaceum*), which belongs to the Sapindaceae family, is a tropical fruit that is easily found in Southeast Asia, the consumption of this rambutan fruit is only eaten by the fruit while the skin of the fruit causes high production of agricultural waste (Lee *et al.,* 2017). There is very little reuse of agricultural waste such as rambutan peel. Therefore, this research focuses on the utilization of rambutan peel waste as an adsorbent. This rambutan peel will be used as hydrochar prepared using the hydrothermal carbonization (HTC) method (Chowdhury *et al.,* 2018). Generally, for the HTC process by adding dry biomass and water into a closed system. Advantages of the HTC process produce dry lignocellulosic biomass with a high carbon content (Kambo and Dutta, 2015). Therefore, rambutan peel hydrochar has the potential to form composites with double hydroxides.

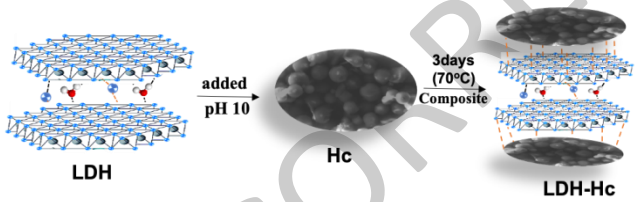

Figure 2. Ilustration Modified LDH-Hc.

LDH or Layered double hydroxide (LDH) is a hydrotalcite material with distinctive characteristics, namely having a large surface area but cannot be used commercially. So it is necessary to modify the material to form a strong structure so that it can be used repeatedly. Lafi *et al.* (2015) (Lafi *et al.,* 2015) conducted a study on Mg-Al LDH which was used to study the adsorption of liquid waste containing congo red dye with a maximum capacity of 111.11 mg/g. Based on research Harizi *et al.* (2018) (Harizi, Chebli, and Bouguettoucha, 2018) reported that modifying Mg-Al-LDH into Mg-Al-Cu-Fe-LDH composite which was applied as an adsorbent for the adsorption of Acid Red 66 with a maximum capacity of 12.22 mg/g and increased in composites reaching 93.12 mg/g. Ni/Al LDH composited with graphite to form Ni/Al-GF and composited with biocar to form Ni/Al-BC which was used to adsorb Congo red which reached a maximum capacity of 116.297 mg/g and 312.50 mg/g reported in (Siregar *et al.,* 2021).

The research is focused on forming LDH composites with rambutan peel hydrochar (with illustrations according to Figure 2) then analyzed using XRD, FT-IR and SEM and will be applied to remove congo red by studying the effect of selectivity of dye mixture, adsorption regeneration, isotherm and adsorption thermodynamics.

2. Materials and methods

2.1. Materials

The chemicals needed in this research for the manufacture of synthetic materials are Nickel (II) nitrate (MW= 290.81 g/mol), aluminum (III) nitrate (MW= 375.13 g/mol), hydrochloric acid/ HCl(MW = 36.458 g/mol), NaOH (MW= 40.00 g/mol) by Sigma Aldrich and Merck. Hydrochar uses precursors from dry rambutan peel that has been dried at a temperature of 105°C for 12 hours. along with procion red, methylene blue, methyl red, congo red, and rhodamine-B dyes as adsorbates in the adsorption study process.

2.2. Methods

2.2.1. Hydrochar preparation by hydrothermal carbonization method

Hydrothermal carbonization method used for the preparation of rambutan peel hydrochar. This method is an aqueous carbonization method at elevated temperature and pressure and uses a stainless steel autoclave hydrothermal tool. A total of 3 g of rambutan peel powder was added to 50 mL of demineralized water, then closed tightly and in an oven at 250℃ for 10 hours. after being baked, the autoclave is cooled and the resulting product is filtered using a vacuum. The black solid resulting from hydrothermal carbonization, called hydrochar, was dried at 105℃ for 24 hours to dry.

2.2.2. Layer double hydroxide synthesis by coprecipitation method

NiAl LDH was prepared by coprecipitation method (Liu *et al.,* 2017) with the following procedure: 100 mL $Ni(NO_3)_2{\cdot}3H_2O$ was mixed with 100 mL $Al(NO_3)_3.9H_2O$ (ratio molar 3:1) then stirred until homogeneous and added slowly with 2 M NaOH (pH 10) and maintained at 80℃ for 17 hours. The final, the suspension was filtered by vacuum, rinsed with demineralized water, then dried at 50℃ for one day, and then the material was grinded and sieved.

2.2.3. Composite LDH-hydrochar preparation

Preparation of NiAl LDH into LDH-Hydrochar composite using coprecipitation method with the following method: 30 mL $Ni(NO_3)_2{\cdot}3H2O$ mixed with 30 mL $Al(NO_3)_3.9H_2O$ (ratio molar 3:1) then dripped with 2 M NaOH solution slowly to pH 10 and maintained for 1 hour. The suspension 3 grams of hydrochar powder was added, stirred for three days at 80°C. The resulting product is filtered, rinsed with demineralized water, and dried at dry temperature, then the material was grinded and sieved.

2.2.4. Adsorption study

2.2.4.1. Adsorption selectivity

The adsorption selectivity process was carried out by mixing cationic and anionic dyestuffs. The dyes are procion red, methylene blue, methyl red, congo red, and rhodamine-B using a concentration of 8 mg/L and add 0.1 g of adsorbent and stirred with time variations (0, 10, 40, 80, and 100 minutes). The final process, the mixture is separated by centrifugation method so that the filtrate and residue separate and facilitate measurement with a UV-Vis spectrophotometer.

2.2.4.2. Adsorbent Reuse

After obtaining selective dye, the process of reusing the adsorbent for the adsorption process was tested for its effectiveness in adsorption of color. In this process, 50 mL of dye is adsorbed and 1 gram of adsorbent is added, then shaken for 3 hours and separated by centrifugation method, the residue is taken and measured using a UV-Vis spectrophotometer, while the residual filtrate is dried and will be reused in the adsorption process. However, before the process of reusing the adsorbent, it must go through a desorption process which is carried out by adding water and ultrasonically for 3 hours. Adsorbent after desorption process was dried and then used repeatedly for the adsorption process, then repeated with the same procedure until it reached a low adsorption effectiveness.

2.2.4.3. Effect of adsorption variation and concentration

The effect of concentration and temperature was used to determine the isotherm analysis data and adsorption thermodynamics. This experiment was carried out by varying the initial concentration of congo red (CR) (25, 50, 75, 100 and 125) mg/L taken as much as 50 mL and added 0.05 grams of adsorbent then shaken for 2 hours with variations in temperature (30, 40, 50, and 60 °C). The mixture was separated by centrifugation method, then the residue was measured using a UV-Vis Spectrophotometer.

2.2.5. Characterization

XRD analysis was performed using the Rigaku Miniflex-6000. Each sample was scanned at 2° sec-1 in the diffraction angle range of 5-70°. X-ray wavelength radiation (λ) is calibrated using alumina. The sample holder has a rotor, which allows sample rotation, to minimize preferential orientation. In the Rigaku apparatus usually use Cu Kα operated at 40 kV and 20 mA. The FTIR spectrum was obtained using a Shimadzu Prestige-21 instrument. Before the sample was analyzed, the sample was added with KBr to remove the water content in the sample, previously calcined at 623 K. For each analysis, a scan was performed for the sample in the wavenumber range of 4000 to 300 cm^{-1}. The BET analysis spectrum was obtained using Quantachrome Instruments. Before the samples were analyzed the samples were calcined at 300 C for 3 hours. For each analysis, scans were carried out with nitrogen gas at 77 K.

3. Results and discussion

The diffractogram of Ni/Al LDH, Hydrochar, and Ni/Al-Hc composites was shown in Figure 3. The diffraction pattern of Ni/Al-Hc as diffraction from Ni/Al LDH and hydrochar. For Ni/Al LDH material has main elements at angles of 2θ = 10.9°, 22.3°, 34.5°, 38.6° and 45.5° with diffraction fields respectively (003), (006), (012), (015) and (018) (JCPDS 40-0216) which indicate the typical structure of hydrotalcite and 2θ = 62.8°,63.9° which indicate the presence of anions between the LDH layers (Gu *et al.,* 2019; Marques *et al.,* 2020). The Ni/Al-Hc composite had an accepted pattern of Ni/Al LDH intensity decreased due to the state of the hydrochar. The wide peak at the diffraction angle of 22° with the diffraction plane (002) indicates the presence of hydrochar in the Ni/Al-Hc composite (Li *et al.,* 2020).

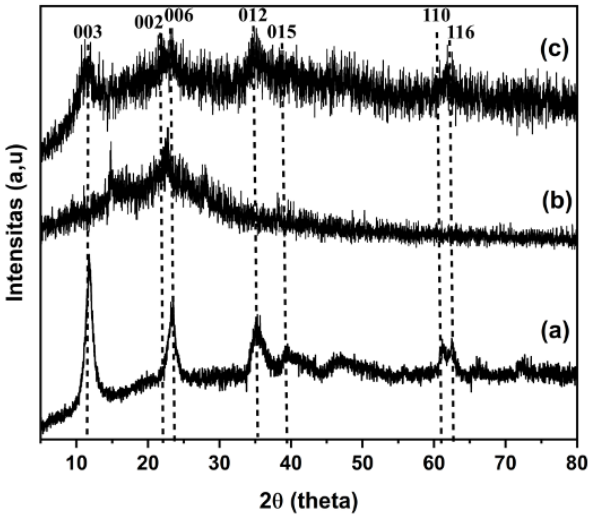

Figure 3. Diffraction patterns of Ni/Al-LDHs (a), Hc (b), Ni/Al-Hc (c).

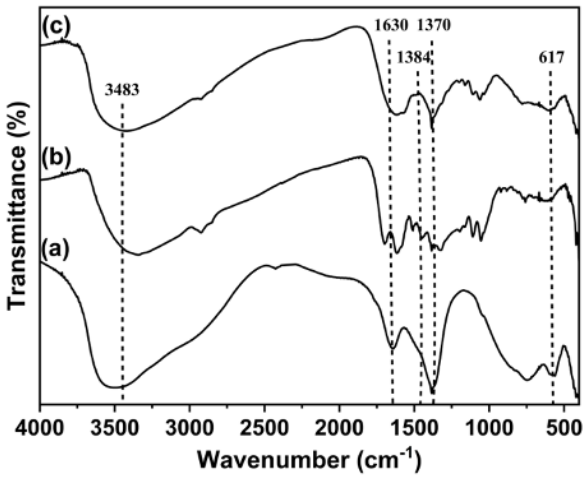

Figure 4. Spectrum FT-IR of Ni/Al-LDHs (a), Hc (b), Ni/Al-Hc (c).

The FTIR spectrum of LDH, Hydrochar, and composites is presented in Figure 4. Figure 4a shows Ni/Al LDH which has a major vibration peak at 3483cm^{-1}(υ O-H stretching) and a vibration peak at 1630cm^{-1}(υ O-H bending). Vibration at 1370cm^{-1}(υ CO_3) and a peak vibration range of 700-400cm^{-1}(υ M-O) (Gu *et al.,* 2019). Hydrochar is shown in Figure 4b, which has a major vibration peak around 617cm^{-1}(υ C-O), 1384cm^{-1}(υ C=C). Figure 4c shows a Ni/Al-Hc having similar vibrations to LDH and hydrochar,

showing various vibrational peaks confirming the successful preparation of LDH/Hc composites.

Figure 5 shows a graphic profile of the adsorption-desorption isotherm of Ni/Al, hydrochar and Ni/Al-Hc composites. The results of the analysis in Figure 5 show that the hydroxy double layer of Ni/Al, Hc, and Ni/Al-Hc composites classified in IUPAC are more inclined to type IV isotherms in the presence of multilayer and hysteresis phenomena.

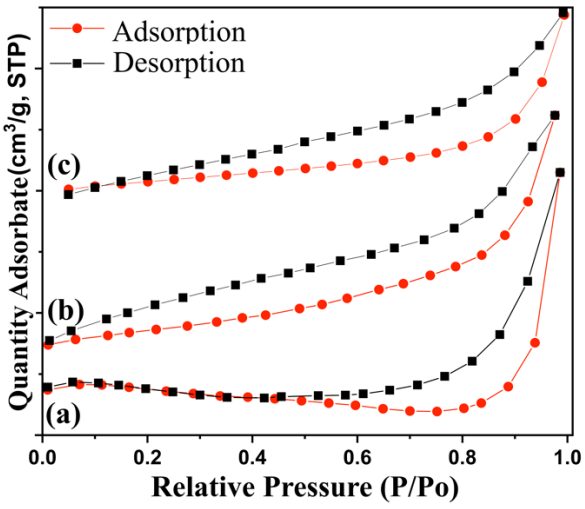

Figure 5. Adsorption-desorption N2 on to the Ni/Al-LDHs (a), Hc (b), Ni/Al-Hc (c).

Based on the literature of (Moller and Pich, 2017) type IV isotherms have a pore size of about 1.5–100 nm and is typical for mesoporous materials. Hysteresis in the LDH of Ni/Al and Ni/Al-Hc composites showed that the hysteresis loop belongs to the H2 type. Type H2, which has a wide loop, has a different desorption curve and looks steeper than the adsorption curve and This H2 loop has a heterogeneous pore structure with sizes ranging from 2-6 nm. Thus, there is a difference in adsorption-desorption because it has a heterogeneous size due to the smaller pore blockage, the desorption branch is steeper, while hysteresis in hydrochar belongs to the H3 type. Type H3 has the same shape between the adsorption and desorption branches. Type H3 indicates that the material has a non-rigid aggregate. Specific surface area, pore diameter and pore volume resulting from measurements of nitrogen adsorption-desorption isotherms are shown in Table 1.

Table 1. BET Surface Area Analysis of Ni/Al-LDH, Hc and Ni/Al-Hc

Materials	Surface area (m^2/g)	Pore volume (cm^3/g)	Pore diameter (nm)
Ni/Al-LDHs	5.845	0.004	4.546
Hc	7.366	0.008	3.189
Ni/Al-Hc	11.879	0.013	2.205

Based on Table 1, the information obtained is Ni/Al-LDH material has a surface area of 5.845 m^2/g, hydrochar has a surface area of 7.366 m^2/g. Table 1 shows that the Ni/Al-hydrochar composite has a larger surface area than the pure material, which is 11.879 m^2/g. These data indicate an increase in the specific surface area of Ni/Al-LDH after being composited with hydrochar.

Selectivity studies of CR, MO, MB, Rh-B, and MG dyes using Ni/Al-LDH, Hc, and Ni/Al-Hc adsorbents were measured with a wavelength range of 400-700 without using the influence of pH. The results of the wavelength scan are shown in Figure 6 shows that the absorbance at the wavelength decreased with the duration of adsorption contact time at 120 minutes showed that among the MB, MG, Rh-B, CR and MO dyes it was seen that CR was more adsorbed using each adsorbent. The decrease in the 120 minutes with Ni/Al-LDH adsorbent reached an adsorbed concentration of up to 8.134 mg/g, while Ni/Al-LDH and HC reached 4.912 mg/g and 6.536 mg/g, respectively. After knowing the most selective CR dye, then CR will be used as an adsorbate to proceed to adsorption kinetics, isotherm adsorption processes and thermodynamic adsorption, desorption and regeneration.

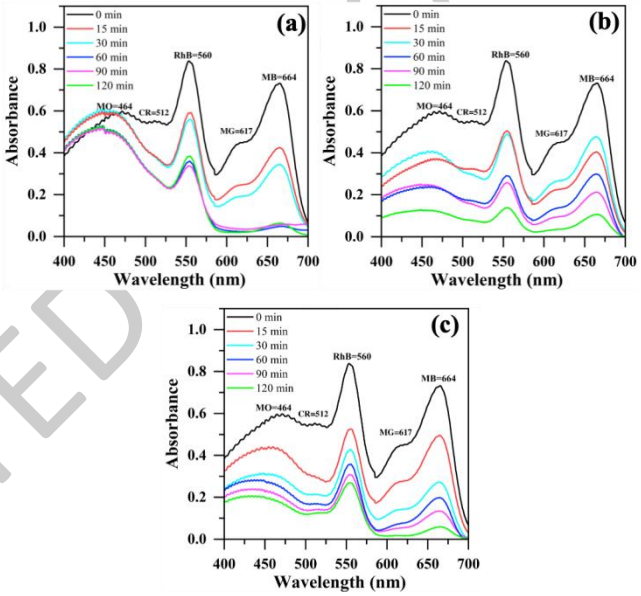

Figure 6. UV-Visible spectra in the range 400-700 nm, a) Ni/Al-LDH, b) Hc, c) Ni/Al-Hc.

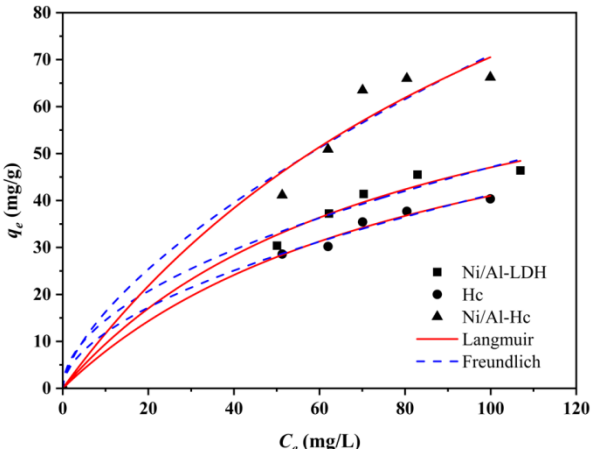

Figure 7. Adsorption isotherm model of CR using Ni/Al, Hc, Ni/Al-Hc.

The effect of adsorption concentration and temperature is shown in Figure 7. Figure 7 shows that the adsorbed CR concentration increased with the addition of the initial concentration of CR used, and the Ni/Al-Hc composite

showed that the adsorbed CR was higher than Ni/Al-LDH and Hc. The adsorption isotherm parameters studied through the Langmuir models and Freundlich models (Ezzati, 2020) are shown in Table 2.

Table 2 presents the parameter data for adsorption isotherms using the Langmuir equation in the form of kL and qm, and Freundlcih in the form of n and kF. From Table 2 it can be concluded that CR adsorption using several adsorbents will tend to follow the Freundlich isotherm followed by a linear regression value close to 1 (R^2> 0.999) with a positive constant n (1.361-5.988) which indicates that adsorption tends to occur by physisorption with physical interactions (Obaid, 2020). Freundlich isotherm is an adsorption process that takes place physically by following the adsorption to form an adsorbate with multilayer (Mittal, Kurup, and Mittal, 2007). The maximum capacity (q_m) seen from the Langmuir constant shows that the Ni/Al-Hc has a large Q_m of 246.23 mg/g, while Ni/Al reaches 61.728 mg/g and hc reaches 69.444. This is supported by the data on the characterization of BET with a specific surface area of Ni/Al-Hc composite which is larger than that of Ni/Al and Hc, Therefore, the adsorption capacity will be greater if the interaction process will be more and more.

Table 2. Isotherm model of CR adsorption on Ni/Al, Hc, Ni/Al-Hc

Materials	Langmuir		Freundlich	
	q_m (mg/g)	kL	n	kF
Ni/Al-LDH	61.728	0.190	5.988	9.471
Hc	69.444	0.166	4.638	7.631
Ni/Al-Hc	246.23	0.096	1.361	3.1290

Furthermore, the calculation of thermodynamic parameter data in the form of Gibbs free energy (ΔG), enthalpy (ΔH), and entropy (ΔS). The thermodynamic data of Ni/Al-LDH, Hc, and Ni/Al-Hc adsorption are shown in Table 3. Table 3 shows the results of calculating the value of Gibbs free energy, enthalpy and entropy. The negative Gibbs free energy (ΔG) value indicates that the adsorption process takes place spontaneously, does not require energy and the adsorption is carried out well at high temperatures. The enthalpy (ΔH) value shows the range of 17.714 kJ/mol to 24.747 kJ/mol which is related to the physical adsorption process and the endothermic reaction (Nimibofa *et al.,* 2017). The positive entropy value (ΔS) is related to the degree of disorder of the adsorbate particles during the adsorption process on the surface of the adsorbent. (Obaid, 2020; Wijaya *et al.,* 2021).

Table 3. Thermodynamic energy data of rambutan peel, Hc, Ni/Al-Hc, Cu/Al-Hc, and Zn/Al-Hc

Parameters	T (K)	Materials		
		Ni/Al-LDH	Hc	Ni/Al-Hc
ΔG°	303	-0.236	0.545	-0.297
	313	-1.061	-0.022	-0.986
	323	-1.885	-0.588	-1.675
	333	-2.710	-1.155	-2.365
ΔS°		0.082	0.069	0.057
ΔH°		24.747	20.583	17.714

Figure 8 shows the study of CR adsorption kinetics using Ni/Al-LDH, Hc, and Ni/Al-Hc. It can be seen in Figure 8 that the Ni/Al-Hc composite has a higher adsorbed concentration than Ni/Al and Hc at 90 minutes. The adsorption kinetics was determined using the Pseudo first order and pseudo second order equations. The parameters are shown in Table 4. Based on Figure 8 and Table 4, CR adsorption using Ni/Al-LDH, Hc, and Ni/Al-Hc tends to follow pseudo first order with a linear regression value that is closer to 1 (R^2> 0.878). According to Simonin (2016) and Kowanga *et al.* (2016) pseudo-first order follows physical adsorption with only one adsorption effect between the adsorbent or adsorbate, this is due to the fact that the interaction between the adsorbent and the adsorbate only occurs physically.

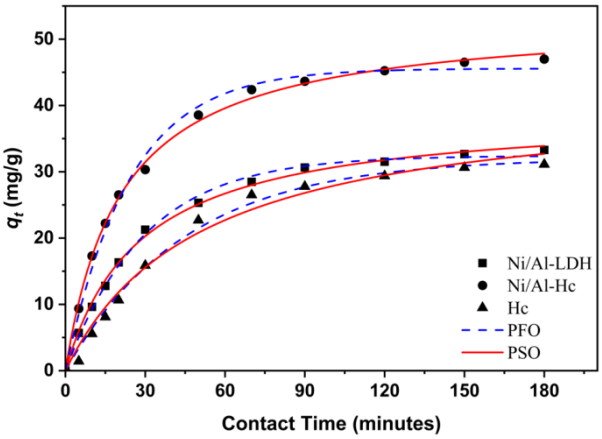

Figure 8. Kinetic models of Ni/Al, Hc, and Ni/Al-Hc.

Figure 9 shows that the desorption of water, hydrochloric acid, sodium hydroxide and ethanol. desorption showed that the desorption process using hydrochloric acid reagent was the most suitable for the CR dye desorption process for each adsorbent reaching 35.26% for Ni/Al-LDH, 32.18% for Hc, and 71.68% for Ni/Al-Hc. This is because hydrochloric acid in water will be ionized into H^+ and Cl^- so that ion exchange occurs and the active site on the adsorbent will be protonated so that the interaction with the adsorbate will weaken, then H+ ions will replace the adsorbate position. Therefore, hydrochloric acid reagent achieves the highest percentage of desorption so that it is most suitable for use in the desorption process (Ivanets *et al.,* 2021; Mishra, 2014).

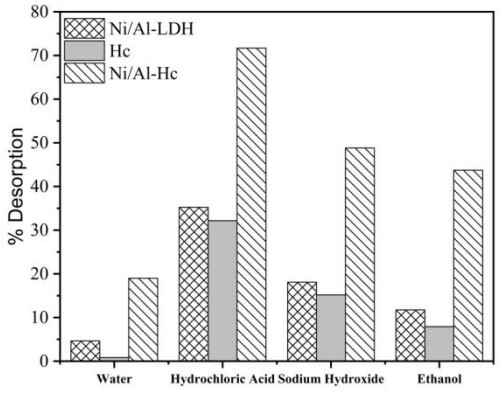

Figure 9. Desorption process using Ni/Al, Hc, and Ni/Al-Hc.

Ni/Al-LDH, Hc, and Ni/Al-Hc showed the ability of recycling adsorption (Figure 10). Ni/Al-LDH has a material capacity to adsorb CR of 78.58% (Cycle I) and decreased to 1.2% (Cycle V). Hc reached 84.97% (Cycle I) and decreased to 4.23% (Cycle V). The results of the regeneration of the Ni/Al-Hc composite adsorbent showed stability up to the third cycle. cycle I Ni/Al-Hc reached 92.69% and decreased by 87.11%; 78.03%; 74.12% and 34.29% up to cycle V. The material without modification experienced a decrease in adsorption ability, while the Ni/Al-Hc composite was more stable. it can be concluded that Ni/Al-Hc has more ability for repeated adsorption processes. The efficiency of adsorbent rate compare with previously reported research papers can be seen in Table 5. Based on the data in Table 5, it can be seen that Ni/Al-Hc has a higher adsorption capacity compared to other adsorbents, thus it can be said that is a potential material that can be used in removing CR.

Table 4. Kinetic parameter of CR adsorption on Ni/Al, Hc , Ni/Al-Hc

Adsorbent	$Qe_{experiment}$ (mg/g)	PFO			PSO		
		Qe_{Calc} (mg/g)	R^2	*k1*	Qe_{Calc} (mg/g)	R^2	*k2*
Ni/Al-LDH	31.111	33.674	0.992	0.025	26.234	0.878	0.222
Hc	33.291	29.600	0.993	0.025	39.370	0.998	0.0008
Ni/Al-Hc	46.984	40.003	0.990	0.028	51.282	0.991	0.001

Table 5. Adsorption Capacity of CR by several Adsorbents

Adsorbents	Adsorption Capacity (mg/g)	References
Litchi seeds powder	20.49	(Edokpayi & Makete, 2021)
Fe_3O_4/NiO	210.78	(Koohi *et al.,* 2021)
Wet-torrefied microalgal biochar	164.35	(Yu *et al.,* 2021)
Magnesium aluminate nanoparticles	24.5	(Tatarchuk *et al.,* 2019)
Polyvinyl alcohol/melamine-formaldehyde composite	221.43	(Bhat *et al.,* 2020)
Decorated graphene with aluminum fumarate metal organic framework	178.57	(Azhdari *et al.,* 2019)
$ZnFe_2O_4/SiO_2$/Tragacanth gum magnetic nanocomposite	159.90	(Etemadinia *et al.,* 2019)
Mg/Fe-CTAB-Layered double hydroxide nanoparticles onto sewage sludge	163.6	(Faisal *et al.,* 2022)
Cu-Ca-Al-layered double hydroxide modified by itaconic acid	84	(Shabani & Dinari, 2021)
Chitosan modified hybrid nanocomposite	104.6	(Ahmad & Ansari, 2021)
Ni/Al-Hc	246.23	This Study

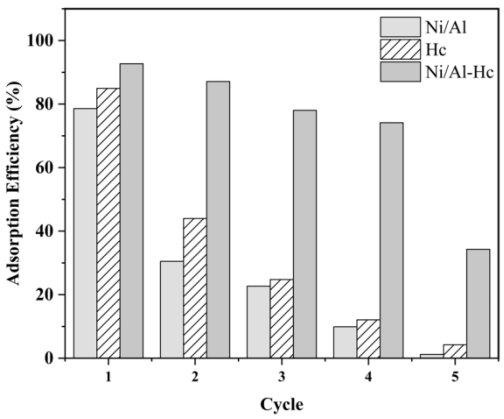

Figure 10. Ni/Al, Hc, and Ni/Al-Hc adsorbent regeneration ability.

4. Conclusion

In this study, Ni/Al was modified with hydrochar from rambutan peel and applied as an adsorbent for Congo red. The success of the synthesis of Ni/Al-Hc composites was proven by the characterization of XRD, FT-IR, BET, and SEM. The adsorption results showed that Ni/Al, Hc and Ni/Al-Hc showed good dye-selective abilities for congo red from the mixed dye adsorption selectivity process. The adsorption ability of congo red was balanced at 100 minutes with a tendency for adsorption to follow pseudo first order, the adsorption isotherm shows that the adsorption of Congo red tends to follow Freundlich with q_m (adsorption capacity) reached 246.23 mg/g, the adsorption process takes place by spontaneous and endothermic, and stable regeneration until the fourth cycle for Ni/Al-Hc.

Acknowledgement

This research was thanks to the research group of Inorganic Materials and Complexes, Faculty of Mathematics and Natural Sciences Sriwijaya University and PDUPT 2021–2022 DIKTI contact No.150/SP2H/LT/DRPM/2021 for additional output research.

References

Adebayo G.B., Mohammed A.A., and Sokoya S.O.. (2016). Biosorption of Fe (II) and Cd (II) Ions from Aqueous Solution Using a Low Cost Adsorbent from Orange Peels, *Journal of Applied Sciences and Environmental Management*, **20**(3), 702.

Adeyemo, *et al.* (2017). Adsorption of Dyes Using Different Types of Clay: A Review, *Applied Water Science,* **7**(2), 543–568.

Ahmad R., and Ansari K. (2021). Comparative study for adsorption of congo red and methylene blue dye on chitosan modified hybrid nanocomposite. *Process Biochemistry*, **108**(3), 90–102.

Azhdari R., *et al.* (2019). Decorated graphene with aluminum fumarate metal organic framework as a superior non-toxic agent for efficient removal of Congo Red dye from wastewater. *Journal of Environmental Chemical Engineering*, **7**(6), 103437.

Ayu, *et al.* (2020). Activated Carbon Preparation from Durian Peel Wastes Using Chemical and Physical Activation Activated Carbon P, A*IP Conference Proceedings,* 2230.

Bhat S.A., *et al.* (2020). Efficient removal of Congo red dye from aqueous solution by adsorbent films of polyvinyl alcohol/melamine-formaldehyde composite and bactericidal effects. *Journal of Cleaner Production*, **255**, 120062.

Chisutia, *et al.* (2014). Adsorption of Congo Red Dye from Aqueous Solutions Using Roots of Eichhornia C, rassipes: Kinetic and Equilibrium Studies, *Energy Procedia*, **50**, 862–869.

Chowdhury, Z.Z., *et al.* (2018). Effect of Temperature on the Physical, Electro-Chemical and Adsorption Properties of Carbon Micro-Spheres Using Hydrothermal Carbonization Process, *Nanomaterials*, **8**(8), 1–19.

Devi, V.S. *et al.* (2020). Materials Today : Proceedings Adsorption of Congo Red from Aqueous Solution onto Antigonon Leptopus Leaf Powder : Equilibrium and Kinetic Modeling, *Materials Today: Proceedings*, **26**(2), 3197–3206.

Edokpayi J.N., and Makete E. (2021). Removal of Congo red dye from aqueous media using Litchi seeds powder: Equilibrium, kinetics and thermodynamics. *Physics and Chemistry of the Earth*, **123**(1), 103007.

Etemadinia T., Barikbin B., and Allahresani A. (2019). Removal of congo red dye from aqueous solutions using znfe2o4/sio2/Tragacanth gum magnetic nanocomposite as a novel adsorbent. *Surfaces and Interfaces*, **14**(10), 117–126.

Ezzati, R. (2020), Derivation of Pseudo-First-Order, Pseudo-Second-Order and Modified Pseudo-First-Order Rate Equations from Langmuir and Freundlich Isotherms for Adsorption, *Chemical Engineering Journal*, **392**(9), 123705.

Faisal A.A.H., *et al.* (2022). Precipitation of (Mg/Fe-CTAB) - Layered double hydroxide nanoparticles onto sewage sludge for producing novel sorbent to remove Congo red and methylene blue dyes from aqueous environment. *Chemosphere*, **291**(1), 132693.

Gu, Z. *et al.* (2019). An Aluminum Silicate Modified Ni-Al LDHs Film to Improve the Corrosion Resistance of AZ31 Mg Alloy, *Materials Letters*, **252**(2019), 304–307.

Harizi, *et al.* (2018). A New Mg – Al – Cu – Fe-LDH Composite to Enhance the Adsorption of Acid Red 66 Dye : Characterization, Kinetics and Isotherm Analysis, *Arabian Journal for Science and Engineering,* **44**, 5245–5261.

Ivanets, A. *et al.* (2021). Effect of Mg2+ Ions on Competitive Metal Ions Adsorption/Desorption on Magnesium Ferrite: Mechanism, Reusability and Stability Studies, *Journal of Hazardous Materials*, **411**(12), 1–9.

Kambo, H.S., and Dutta A. (2015). A Comparative Review of Biochar and Hydrochar in Terms of Production, Physico-Chemical Properties and Applications, *Renewable and Sustainable Energy Reviews*, **45**, 359–378.

Koohi P., Rahbar-kelishami A., and Shayesteh H. (2021). Efficient removal of congo red dye using Fe3O4/NiO nanocomposite: Synthesis and characterization. *Environmental Technology and Innovation*, **23**, 101559.

Kowanga K.D., Gatebe E., Mauti G.O., and Mauti E.M. (2016). Kinetic, sorption isotherms, pseudo-first-order model and pseudo-second-order model studies of Cu(II) and Pb(II) using defatted Moringa oleifera seed powder. *The Journal of Phytopharmacology*, **5**(2), 71–78.

Lafi, R. *et al.* (2015). Adsorption Study of Congo Red Dye from Aqueous Solution to Mg – Al – Layered Double Hydroxide, *Advanced Powder Technology Journal,* **27**(1), 232–237.

Lee, H-j. *et al.* (2017). Immobilization Of Rambutan (Nephelium Lappaceum) Peel As A Sorbent for Basic Fuchsin Removal, *Environment Protection Engineering,* **43**(1), 1.

Li, J. *et al.* (2020). Pyrolysis Behavior of Hydrochar from Hydrothermal Carbonization of Pinewood Sawdust, *Journal of Analytical and Applied Pyrolysis*, **146**(12), 104771.

Li, S. *et al.* (2020). Adsorption and Mechanistic Study of the Invasive Plant-Derived Biochar Functionalized with CaAl-LDH for Eu(III) in Water, *Journal of Environmental Sciences (China)*, **96**(1), 127–137.

Litefti, *et al.* (2019). Adsorption of an Anionic Dye (Congo Red) from Aqueous Solutions by Pine Bark, *Scientific Reports,* **9**(1), 1–11.

Liu, Huili *et al.* (2017). Ultrathin Ni-Al Layered Double Hydroxide Nanosheets with Enhanced Supercapacitor Performance, *Ceramics International*, **43**(16), 14395–1400.

Ma, J. *et al.* (2021). Modified Fruit Pericarp as an Effective Biosorbent for Removing Azo Dye from Aqueous Solution: Study of Adsorption Properties and Mechanisms, *Environmental Engineering Research*, **27**(2), 200634.

Marques, B.S. *et al.* (2020). Ca–Al, Ni–Al and Zn–Al LDH Powders as Efficient Materials to Treat Synthetic Effluents Containing o-Nitrophenol, *Journal of Alloys and Compounds*, **838**(2020), 155628.

Mishra S. *et al.* (2020) Cobalt ferrite nanoparticles prepared by microwave hydrothermal synthesis and adsorption efficiency for organic dyes: isotherms, thermodynamics and kinetic studies. *Advanced Powder Technology*, **31**(11), 4552–4562.

Mishra S.P. (2014). Adsorption–Desorption of Heavy Metal Ions. *Current Science,* **107**(4), 601–612.

Mittal, *et al.* (2007). Freundlich and Langmuir Adsorption Isotherms and Kinetics for the Removal of Tartrazine from Aqueous Solutions Using Hen Feathers, *Journal of Hazardous Materials*, **146**(1–2), 243–248.

Moller, M., and Pich A. (2017). Development of Modified Layered Silicates with Superior Adsorption Properties for Uptake of Pollutants from Air and Water.

Nazal, Mazen K. (2019). Marine Algae Bioadsorbents for Adsorptive Removal of Heavy Metals, *Advanced Sorption Process Applications*, 1–14.

Nimibofa, *et al.* (2017). Comparative Sorption Studies of Dyes and Metal Ions by Ni/Al-Layered Double Hydroxide, *International Journal of Materials and Chemistry*, **7**(3), 25–35.

Normah *et al.* (2021). Competitive Removal of Cationic Dye Using NiAl-LDH Modified with Hydrochar, *Ecological Engineering & Enviromental Technology*, **22**(4), 124–135.

Obaid, S.A. (2020) Langmuir, Freundlich and Tamkin Adsorption Isotherms and Kinetics for the Removal Aartichoke Tournefortii Straw from Agricultural Waste, *Journal of Physics: Conference Series*, **1664**(1), 012011.

Olusegun, S.J, and Mohallem N.D.S. (2020). Comparative Adsorption Mechanism of Doxycycline and Congo Red Using Synthesized Kaolinite Supported CoFe2O4 Nanoparticles, *Environmental Pollution*, **260**, 114019.

Palapa, N.R. *et al.* (2021). Biochar from Rice Husk as Efficient Biosorbent for Procion Red Removal from Aqueous Systems, *Applied Environmental Research*, **43**(3), 79–91.

Satya, A. *et al.* (2020). Batch Study of Cadmium Biosorption by Carbon Dioxide Enriched Aphanothece Sp. Dried Biomass, *Water (Switzerland)*, **12**(1), 264.

Shabani S., and Dinari M. (2021). Cu-Ca-Al-layered double hydroxide modified by itaconic acid as an adsorbent for anionic dye removal: Kinetic and isotherm study. *Inorganic Chemistry Communications*, **133**(7), 108914.

Simonin, J.P. (2016). On the Comparison of Pseudo-First Order and Pseudo-Second Order Rate Laws in the Modeling of Adsorption Kinetics, *Chemical Engineering Journal*, **300**, 254–263.

Siregar, P.M.S.B.N., *et al.* (2021). Structural Stability of Ni/Al Layered Double Hydroxide Supported on Graphite and Biochar Toward Adorption of Congo Red, *Science and Technology Indonesia*, **6**(2), 85–95.

Tatarchuk T., *et al.* (2019). Removal of Congo Red dye, polar and non-polar compounds from aqueous solution using magnesium aluminate nanoparticles. *Materials Today: Proceedings*, **35**, 518–522.

Viena V., Elvitriana, and Nizar M. (2019). Characterization of Activated Carbon Prepared from Banana Peels: Effect of Chemical Activators on the Adsorption of Gas Emissions. *Journal of Physics: Conference Series*, **1232**(1), 012005.

Wijaya, A. *et al.* (2021), Innovative Modified of Cu-Al / C (C = Biochar , Graphite) Composites for Removal of Procion Red from Aqueous Solution, *Science and Technology Indonesia,* **6**(4), 228–234.

Xie, Z. *et al.* (2014). Production of Biologically Activated Carbon from Orange Peel and Landfill Leachate. *Subsequent Treatment Technology*, **6**, 1–10.

Yu K.L., *et al.* (2021). Adsorptive removal of cationic methylene blue and anionic Congo red dyes using wet-torrefied microalgal biochar: Equilibrium, kinetic and mechanism modeling. *Environmental Pollution*, **272**, 115986.